2D Host-Guest Supramolecular Chemistry for on-Monolayer Graphene Emitting Platform

Byeonggwan Kim, Cheolhyun Cho, Imad Arfaoui, Céline Paris, Christophe Petit, Tangui Le Bahers, Eunkyoung Kim, André-Jean Attias

2D Host-Guest Supramolecular Chemistry for on-Monolayer Graphene Emitting Platform.

Byeonggwan Kim[acd], Cheolhyun Cho[b], Imad Arfaoui[c], Céline Paris[c], Christophe Petit[c], Tangui Le Bahers[ae], Eunkyoung Kim[ab]*, and André-Jean Attias[a]*

[a] Building Blocks for FUture Electronics Laboratory, UMI 2002, CNRS-Sorbonne Université-Yonsei University, Yonsei University, 50 Yonsei-ro, Seodaemun-gu, 03722 Seoul, Korea
E-mail: andre-jean.attias@cnrs.fr; eunkim@yonsei.ac.kr

[b] Department of Chemical and Biomolecular Engineering, Yonsei University, 50 Yonsei-ro, Seodaemun-gu, 03722 Seoul, Korea

[c] MONARIS, UMR 8233 CNRS-Sorbonne Université, Sorbonne Université, 4 Place Jussieu, 75252 Paris Cedex, France

[d] IPCM, UMR 8232 CNRS-Sorbonne Université, Sorbonne Université, 4 Place Jussieu, 75252 Paris Cedex, France

[e] Univ Lyon, ENS de Lyon, CNRS, Université Lyon 1, Laboratoire de Chimie UMR 5182, Lyon, France

Keywords: graphene, surface-confined host-guest system, electronic decoupling, nanophotonics, DFT and TD-DFT calculations.

Abstract

Here, is reported a novel strategy of non-covalent functionalization of graphene to avoid the electronic coupling between this semi-metal and directly adsorbed optically active molecules. Graphene-confined supramolecular host-guest recognition is used to elaborate an emitting hybrid platform. It is shown that the cavities of an on-monolayer graphene nanoporous self-assembled network are able to trap zinc phthalocyanine molecules coordinated to an emitting axial ligand. As a result, the emission of the hybrid system exhibits the same features as the isolated molecular emitter, demonstrating that the fluorescence is not quenched by graphene and that the well-controlled inter-chromophore distance prevents any interaction between the dyes. Furthermore, an in-depth modelling study confirms the weak interaction between the out of plane emitting moieties and the monolayer graphene. This work opens a new avenue for the realization of innovative light-responsive graphene-based devices in nanophotonics and optoelectronics.

New Concepts

Electronic decoupling of molecular chromophores from graphene to preserve their optical properties with the objective to elaborate light-responsive hybrid system for new electronic and optoelectronic nanodevices remains largely unexplored. Here, we demonstrate for the first time an easy-to-implement strategy that successfully tackles the electronic decoupling issue. This noncovalent functionalization approach, based on two-dimensional (2D) host-guest supramolecular chemistry, enables immobilization of emitting 3D guest molecules into a 2D self-assembled porous template. The well-controlled graphene-chromophore and inter-chromophore distances combined with the mastered chromophore orientation allow the elaboration of an emitting graphene-based system with the same features as the single molecular emitter, demonstrating the preservation of its intrinsic electronic properties. Therefore, contrary to current photo-active graphene systems that take advantage of the direct electronic interaction (quenching) between the photo-responsive moieties and the graphene, our decoupling strategy that retains the molecular electronic properties is promising to create on demand novel light-responsive 2D materials platforms. This approach should allow the functionalization of graphene with optically active molecules like emitting chromophores but also photoswitchable molecules, the well-controlled distance between photo-active moieties giving sufficient free volume to perform motions. Besides, our decoupling method opens perspectives in the field of single-molecule electroluminescence through scanning tunneling microscope (STM)-induced fluorescence.

1. Introduction

Over the past few decades, supramolecular self-assembly at surfaces has attracted tremendous attention in nanoscience since allowing not only to create well-defined surface-confined two-dimensional (2D) networks, but also to perform on-surface chemistry and to elaborate functional systems.[1-3] Recently, the advent of 2D layered materials as substrates for the self-assembly has opened perspectives for their non-covalent functionalization and the development of hybrid architectures.[4-7] Most studies have focused on self-assembly of planar organic molecules (tectons) lying flat on the surface, leading to hybrid structures where the arising strong in-plane interactions between the adsorbed molecules and the 2D substrates confer new electrical or optical properties.[8-12] However, in the case of the adsorption of photo-responsive molecules on pristine graphene the interaction is detrimental due to the electronic coupling with this transparent semi-metal, responsible e.g. for the fluorescence quenching of directly adsorbed molecular emitters. Thus, preserving the intrinsic optical properties of optically active molecules by the electronic decoupling from graphene substrate is a key issue to develop new light-responsive graphene-based systems.

More generally, the electronic decoupling from a metal substrate is usually achieved by self-assembling three-dimensional (3D) functional tectons,[13, 14] in order to elevate the molecular functionality from the surface, along its normal direction. On the other hand, controlling the orientation of the photosensitive moieties along a preferential direction, for example to align transition or permanent dipole moments, is another issue. However, only a few number of 3D tecton structures have been designed to achieve the decoupling from graphene, suh as a tripodal graphene binder bearing a redox-active functionality,[15] or two-faces 3D building blocks equipped with functional groups.[16] Despite the realization of an emitting graphene-based system,[17] the synthesis of such tectons in large amount for high surface coverage in view of applications in photonics appears tricky on the one hand, and the

orientation of the emitting moiety was not controlled on the other one. Moreover, the emission originated from neighboring dyes groups forming few-dyes clusters. Recently, we showed that metal-ligand coordination and host-guest chemistry on highly oriented pyrolytic graphite (HOPG), a graphene model material, allowed for trapping a 3D zinc phthalocyanine complex into a 2D porous supramolecular network, the ligand projected away from the substrate.[18] Therefore, we expect to tackle the electronic decoupling issue in an easy way, by extending this strategy to graphene as a transparent substrate on the one hand, and to an photoactive axial ligand designed to stay perpendicularly on the other hand. Moreover, thanks to the well-controlled inter-pores distance into the host porous network, any interactions between the molecular emitters should be avoided.

Here, we report the first emitting hybrid platform obtained by combining graphene-confined host-guest recognition and metal-ligand coordination approach. This is achieved by filling the cavities of a host porous network self-assembled on monolayer graphene with emitting guest complex from ZnPc coordinated to an appropriately designed pyridine-functionalyzed perylene tetracarboxydiimide (PTCDI) derivative (ZnPc:Py-PTCDI, Scheme 1). We demonstrate (i) the realization of a 2D array of ~ 2 nm in height of molecular emitters standing-up on the substrate i.e. aligned along the perpendicular direction, and (ii) the emission of the on-graphene platform at the PTCDI core emission wavelength without any aggregation effect. Last but not least, the fact that the graphene substrate does not affect the spectroscopic properties of the PTCDI moity is supported by TD-DFT calculations. All these results validate our strategy effectiveness to tackle the decoupling issue on graphene, opening new perspectives for the realization of new light-responsive graphene-based hybrid systems for nanophotonics and optoelectronics.

2. Results and Discussion

2.1. Synthesis and supramolecular self-assembly

We designed and synthesized in a one-step process an unsymmetrical axial ligand Py-PTCDI (Scheme 1) with a perylene tetracarboxydiimide core as an emitting moiety, an alkyl group at one imide position for the solubility, and a pyridyl group on the other nitrogen atom for later binding to Zn-phthalocyanine (ZnPc). Adapting an one-step protocol developed for the synthesis of unsymmetrical alkyl-PTCDI-aryl derivatives,[19] the reaction of perylene dianhydride with a stoichiometric mixture of 1-hexylheptylamine and 4-aminopyridine afforded the target ligand Py-PTCDI in 23% yield (See Supporting Information for experimental details).

The coordination of ZnPc to the ligand Py-PTCDI was confirmed by UV-Vis spectroscopy, that showed absorption changes of ZnPc in a non-coordinating solvent (toluene) during increasing addition of Py-PTCDI (Figure S1). The observed slight red-shift of the ZnPc Q-band (670 nm) was in good agreement with literature on the one hand,[20] and confirmed by TD-DFT calculations (computed transition at 624 nm before complexation and at 625 nm after complexation) on the other hand. The saturation was reached at about 100 equivalents of Py-PTCDI.

The surface-confined supramolecular host-guest recognition was performed on HOPG and graphene grown by chemical vapor deposition (CVD) and transferred to quartz as substrates. This noncovalent functionalization was carried out in a two-step process (See Experimental Section). The first stage of the deposition protocol consisted in the realization of the 2D porous template. This structure was obtained by the well-mastered self-assembly of an alkoxy-substituted conjugated tristilbene core, TSB12 (Scheme S1), a building block known for forming porous honeycomb networks on HOPG and graphene.[21] In a second step, a solution in toluene of the 3D guest tecton (ZnPc:Py-PTCDI complex) was subsequently drop-casted to immobilize it into the templated 2D network whose pores could accommodate

selectively the ZnPc molecular unit.[22] The excess of molecules was removed by generous rinsing with toluene.

2.2 Characterizations of the surface-confined host-guest system

The challenges are to demonstrate that (i) the complex fills the cavities, (ii) the ~2nm in height ligand stands-up, and (iii) the hybrid systems emits.

2.2.1. Scanning tunneling microscopy (STM). With this aim, molecular organization of the final adlayer was first investigated by STM, at the solid/1-phenyloctane interface. The liquid acts like an infinite reservoir of molecules while providing conditions for observing the interface in a protected environment. Before studying the self-assembly of the host-guest system (TSB12+ZnPc:Py-PTCDI) on graphene, the STM study was carried out on HOPG as a model surface to validate the feasibility and measure some parameters (See Supporting Information for experimental details, Figure S2, S3, and S4). STM reveals that a supramolecular honeycomb network is formed whose cavities are filled with entities forming protrusions with an apparent height distribution ~1.5 ± 0.2 nm. Then, we moved to monolayer graphene as substrate to characterize the targeted functional system. Figure 1a shows a large-scale (300×300 nm^2) STM image, typical of STM characterization at different spots, recorded after drop-casting the ZnPc:Py-PTCDI solution three times. Despite the roughness of the transferred graphene and a possible blurring effect, it was possible to observe an array of white spots as with HOPG (see ESI) and to deduce similar lattice parameters ($a = b$ = 4.2 nm and α = 60°). These results confirm that a host-guest recognition process also occurs on graphene. The adsorption of the ligand in the pores appears unlikely since the conjugated skeleton size (~1.9 nm) without the alkyl chains is roughly equal to the templated network cavity diameter (~1.89 nm).[23] The most important result is the average apparent height, 1.5 ± 0.1 nm (Figure 1b), provided by a deep statistical analysis showing that the Gaussian fitting profile of the apparent height distribution for the bright spots over the whole STM image (Figure 1a). A statistical analysis over the whole STM image also shows a inter-spots distance

a = 4.2± 0.2 nm in accordance with the values measured on HOPG (Figure S3b and S3c). Thus, thanks to the observation of these protrusions we can deduce from large scale STM imaging that the cavities are likely filled with entities projecting from the surface.

2.2.2 UV-Vis and Raman spectroscopy. To go a step forward, Raman spectroscopy was used not only to probe the chemical nature of the protrusions but also to get information about any fluorescence quenching due to coupling with the substrate or transfer to the metallo-phthalocyanine. Preliminarly, the absorption and emission spectra of Py-PTCDI solution in toluene were recorded (Figure S5a) to choose the laser excitation wavelength. Py-PTCDI absorption spectrum exhibits the perylene derivatives typical vibronic feature assigned to 0-0', 0-1', and 0-2' transition energy with absorption bands at 527, 491, and 460 nm, respectively. The fluorescence spectrum of Py-PTCDI excited at 527 nm shows the same behavior (mirror image) with emission peaks at 540, 577, and 627 nm. Regarding the vibronic progression of both absorption and emission spectra, the main distance between component peaks of each spectrum is on average ~0.17 eV (~1370 cm^{-1}). The vibronic nature of the spectra is further confirmed by the simulated vibronically resolved absorption and emission spectra using TD-DFT adiabatic energy transitions. These simulations give a vibronic progression around ~0.18-0.19 eV, thus very close to the exprimental value. The analysis of the computations reveals that the progression comes from two vibrational modes associated to an inplane vibration of H atomes of PTCDI core (computed at 1338 cm^{-1}) and a C=C streching mode of the PTCDI moity (computed at 1677 cm^{-1}) at the electronic excited state. Based on the above optical properties, the Raman spectra were collected using a 532 nm laser excitation wavelength, which is in resonance with Py-PTCDI molecules.

Then, the Raman spectra (Figure S6) of on glass slides drop-casted films of TSB12, ZnPc, and Py-PTCDI were recorded to assign the characteristic vibrational Raman bands. Thus, for Py-PTCDI and in spite of a strong fluorescence, we can clearly see the presence of 3

bands: around 1300 and 1380 cm^{-1} (stretching of the chromophore ring) and around 1580 cm^{-1} (C=C stretching).[24]

In a first stage, we used HOPG as a model substrate for Raman experiments (Figure S7a). Despite a low intensity of the Raman signals and large HOPG bands hiding some Py-PTCDI Raman bands, the results (See Supporting Information and Figure S8) showed that the ZnPc:Py-PTCDI could be trapped into the pores of the host TSB12 network on HOPG.

Then, the Raman study of the host-guest system self-assembly was extended to graphene. The Raman spectrum of the graphene used (Figure S7b) exhibits two typical Raman mode,[25] the G-mode band (1585 cm^{-1}) and the 2D-mode band (2677 cm^{-1}). The latter one, symmetric, is characteristic of a monolayer graphene. Figure 2 shows the evolution of the Raman spectra at each step of the self-assembly of the host-guest platform was investigated in the 1000-1700 cm^{-1} range, where lie the characteristic vibrational Raman bands of TSB12, ZnPc, and Py-PTCDI. First, deposition on graphene of TSB12 molecules (Figure 2b) induces a slighly up-shifted of the G-mode band compared to pristine graphene, from 1585 to 1588 cm^{-1} (Figure 2a). This could be attributed to an interaction between graphene and the organic adlayer. However, no peak from the TSB12-based self-assembled monolayer is detected because we are far from its absorption wavelength (λ_{max} = 314 nm and $\lambda_{tail\text{-}end}$ = 354 nm). Second, after drop-casting of the ZnPc:Py-PTCDI (1:100) solution and rinsing, a fluorescence background is observed, demonstrating that the PTCDI core emission is not quenched by the substrate (Figure 2c and 2e). Third, the two characteristic PTCDI core Raman modes (~1300 and ~1380 cm^{-1}) were clearly detected (Figure 2c to 2f). They are matched to the vibronic coupling (~0.17 eV; ~1370 cm^{-1}) observed on UV-Vis spectra (Figure S5a). Furthermore, the typical Raman mode of PTCDI (~1574 cm^{-1}) assigned to C=C stretching is also now evidenced, unlike on HOPG substrate (Figure S8). Finally, beside the improvement of the Py-PTCDI Raman signals, the intensity of the Raman peaks is also sensitive to the degree of pores filling. Comparison of PTCDI (1300 and 1380 cm^{-1})/graphene (1588 cm^{-1}) Raman peak

intensity ratio shows a ~40 increase after three drop-castings (Figure 2d and 2f). On the other hand, the role of the ZnPc for immobilizing the complex is clearly evidenced in Figure S9 recorded following the drop-casting, on the TSB12 modified substrate, of a Py-PTCDI solution, before and after rinsing. The Py-PTCDI Raman modes, visible just after deposition, completely disappeared after rinsing. All these results confirm that the TSB12-based 2D porous network hosts the ZnPc:Py-PTCDI guest molecules without any coupling between graphene and the molecular emitters.

2.3 Confocal fluorescence microscopy

Finally, the confocal fluorescence microscopy was used to probe the optical features of the self-assembled on-monolayer graphene platform, in terms of orientation as well as excitation and emission spectra of the fluorescent PTCDI core. On the molecular scale, the Py-PTCDI molecule can be described as an oscillating dipole parallel to the long axis.[26] Thus, the spatial distribution of the emission intensity is anisotropic, molecules emitting most light in the direction perpendicular to this dipole. Therefore, depending on the orientation of the targeted on-monolayer graphene platform with respect to the incident laser beam, confocal fluorescence microscopy should help to gain a deeper insight into the molecular emitters orientation. The control of the sample orientation is achieved by rotating the sample (θ = 0 or 45°), as shown on Figure 3a. The excitation laser beam wavelength was chosen equal to 490 nm, a value corresponding to the absorption wavelength of the PTCDI 0-1' energy transition (Table 1 and Figure S5a) and far from the TSB12 and ZnPc absorption wavelengths (314 and 672 nm, respectively). Confocal microscopy images of pristine monolayer graphene on quartz, covered with the TSB12-based self-assembled network, and subsequent addition of ZnPc are reported on Figure S10. As expected, as long as the sample is perpendicular to the incident laser beam (θ = 0°) or tilted (θ = 45°), there is no emission (black images). In contrast, after deposition of the ZnPc:Py-PTCDI complex, if no emission (black image) is observed when the sample is perpendicular to the incident beam (Figure 3b), emission is observed when the

sample is tilted at 45°, the focused area appearing as bright fluorescent spots in the fluorescence confocal microscopy image (Figure 3c). Thus, excitation and emission spectra were recorded for this sample orientation (Figure 3d). Interestingly, both fluorescence excitation and emission spectra exhibited a vibronic profile as in solution on the one hand, and the wavelength values (Table 1) were only slightly blue-shifted on the other hand, mainly because of solvent free measurements. This is different from Py-PTCDI film where the fluorophores aggregation leads to a red-shifted and broad structure-less emission spectrum (Figure S5b).

Despite it is not possible to determine any relative or absolute fluorescence quantum yield of the molecular emitters-based monolayer, Figure 3c and 3d provide qualitative information about the fluorescence efficiency of the emitting hybrid platform. First, the emitting monolayer exhibits a clearly detectable emission; second, the intensity at the maximum of the emission spectrum on Figure 3d is well above (~ 4 orders of magnitude) the threshold of the detector (~ 25 a.u. vs ~0.001 a.u.). All the above results confirm that (i) the PTCDI core is perpendicular to the substrate, (ii) the fluorescence is not quenched by graphene, and (iii) the well-controlled inter-chromophore distance (4.2 nm) prevents any interaction between the dyes.

2.4 Theoretical approach.

The weak interaction between the ZnPc:Py-PTCDI dye and the substrate is further confirmed by DFT and TD-DFT calculations. The ZnPc:Py-PTCDI adsorbed on a graphene surface covered by the TSB12 molecule was simulated using a monolayer of graphene within a unit cell made of a 16×16 graphene supercell covered by a monolayer of TSB12 molecules. Two TSB12 molecules were used per unit cell, in agreement with a previous STM investigation.[23] The relaxation of atomic positions was done first at the tight-binding DFT level and then at the PBE level. The final structure is presented in Figure 4 and given in Supporting Information. The simulation of STM images of the TSB12 molecule adsorbed on

graphene is presented in Figure S11. The agreement between simulated and experimental images supports the quality of our model. In terms of geometry, the distance between pores generated by TSB12 molecules is 4.1 nm, in agreement with the experiment. Geometrical parameters associated to this system are given on **Figure 4b**. The absorption spectra of the ZnPc:Py-PTCDI has been computed for three different situations: (a) in gas phase on a geoemtry optimized in gas phase using the same computational details as for periodic calculation, (b) in gas phase for the ZnPc:Py-PTCDI geometry optimized in the graphene-TSB12 pores and (c) on the ZnPc:Py-PTCDI geometry optimized in the graphene-TSB12 pores surrounded by point charges associated to the TSB12 molecules and graphene layer (see Experimental Section for more details about this calculation). The computed transition energies of the ZnPc and the Py-PTCDI moities are presented in Table 2. We can see that neither the change in geometry induced by the adsorption nor the influence of the electrostatic embedding affect the electronic transitions confirming that the host used to accomodate the molecule ZnPc:Py-PTCDI does not alter its electronic structure.

3. Conclusion

To summarize, we have developed a new strategy to successfully electronically decouple molecular emitters from graphene. This is achieved by using the 2D host-guest supramolecular chemistry for the fabrication by a soft process of an emitting on-monolayer graphene functional platform. This noncovalent graphene functionalization approach allows the immobilization, in a well-defined 2D nanoporous network, of an emitting 3D ZnPc complex that projects a dye-based ligand away from the surface and aligned along the normal direction. Thanks to the resulting electronic decoupling from the graphene, as well as the transition dipole orientation and intermolecular distance control, the hybrid system emits light with the same features as the isolated molecular emitter. The flexibility for the choice of the

ligand functionality combined with the modular ZnPc complexation, and the possibility to extend this noncovalent functionalization strategy to other 2D materials open new perspectives for 2D materials-based nanophotonics applications. This approach should allow the functionalization of graphene with optically active molecules like emitting chromophores but also photoswitchable molecules, the well-controlled distance between photo-active moieties giving sufficient free volume to perform motions. On the other hand, our decoupling method opens perspective in the field of electrically induced luminescence at the single-molecule level through STM tip-induced electrical field.'

4. Experimental section

Materials: All chemicals were purchased from Sigma-Aldrich and used without purification. TSB12 was synthesized according literature procedure.[21] Highly oriented pyrolytic graphite (HOPG, ZYB, 15 mm × 15 mm × 2 mm) was purchased from MaTecK, GmbH. Monolayer graphene grown by CVD processing onto copper foil then transferred onto quartz (1"x1") was purchased from Graphene Supermarket. A 250 μm Pt/Ir (80/20) wire purchased from Goodfellow was mechanically cut to fabricate a tip prior to use for STM measurement.

Characterizations: UV-vis-NIR spectra of Py-PTCDI toluene solution (1.4 μM) and Py-PTCDI film (thickness=~200 nm) on quartz were recorded with a Lambda 750, UV/Vis/NIR Spectrophotometer (PerkinElmer). 1 cm-pathlength quartz cuvette was used for solution measurement. Fluorescence spectra of Py-PTCDI toluene solution (1.4 μM) and Py-PTCDI film (thickness ~200 nm) on quartz were obtained using a luminescence spectrometer (Perkin Elmer, Model LS55). The ^{1}H-NMR spectrum was obtained using a BRUKER ARX-400 spectrometer (400 MHz) with $CDCl_3$ and tetramethylsilane as solvent and internal reference, respectively. STM measurement were performed using Keysight STM scanner working with 5100 AFM/SPM microscope system at room temperature. All experiments were repeated several times with different STM tips at different positions on the sample. Raman

spectroscopy was carried out on a LabRam Aramis spectrometer (Horiba Jovin Yvon) equipped with 532 nm diodes laser, and an 1800 grooves/mm grating that gives a spectral resolution of about 0.65 cm^{-1}. The laser power was set at 0.5 mW at the sample using a 50x objective. Due to the small quantities of molecules deposited on the HOPG surfaces, the acquisition time has been increased to 10 min for the self-assembled monolayers molecules. The integration time was 3 min for the molecules deposited on graphene. Raman spectroscopy for the powders and films was obtained with a LabRam Infinity Spectrometer (Horiba Jovin Yvon) equipped with 532 nm diodes laser, and a 1800 groove/mm grating that gives a spectral resolution of about 1.3 cm^{-1}. The laser power was set at 0.3 mW on the sample using a 50x objective and the integration time was 1 min. The confocal fluorescence microscopy was performed with a Leica TCS SP8 inverted microscope at the Korea Basic Science Institute (KBSI, Western Seoul Center). The photoluminescent (PL) spectra were recorded using a Ocean Optics HR4000CG Composite-grating spectrophotometer with excitation wavelength at 490 nm and a HyD hybrid detector (410–785 nm). The Lambda scans (excitation spectra) and emission spectra were recorded for the sample orientation of 0 and 45° degrees. The spectra from the sample oriented at 45° were compensated according to the depth of field (DoF) equation because of the small focused area at 45 degrees (For more details, see Supporting Information).

STM sample preparation: Atomically clean surface of HOPG was obtained by cleaving the upper graphite layers using the Scotch Tape Method (exfoliation method). After the atomically clean surface were checked by STM under air atmosphere, the molecular monolayers were self-assembled on top of the substrate. TSB12 solution (5 μl, 34 μM, toluene) was drop-casted (~7 × 7 mm^2) onto clean HOPG substrates (1.5 × 1.5 cm^2) and dried for 5 min in the air. The sample was rinsed 3 times with toluene (0.1 mL × 3). ZnPc:Py-PTCDI (1:100) complex solution (2 μl, 1.4 μM of ZnPc and 140 μM of Py-PTCDI, , toluene) was drop-casted (~7 × 7 mm^2) onto a TSB12/HOPG and dried for 5 min in the air. The

sample was rinsed 3 times with toluene (0.1 mL × 3). 1-Phenyl octane (10 μl) was dropped on the sample area for HOPG-phenyl octane (solid-liquid) interface to reduce the noise. The sample was placed on the sample holder for the STM measurements in the air.

Raman sample preparation:

a) HOPG substrate: TSB12 solution (5 μl, 34 μM, toluene) was drop-casted (~7 × 7 mm^2) onto clean HOPG substrates (1.5 × 1.5 cm^2) and dried for 5 min in the air and the sample was rinsed 3 times with toluene (0.1 mL × 3). ZnPc (2 μL, 1.4 μM, toluene) or ZnPc:Py-PTCDI (1:100) complex solution (2 μL, 1.4 μM of ZnPc and 140 μM of Py-PTCDI, toluene) was drop-casted (~7 × 7 mm^2) onto a TSB12/HOPG and dried for 5 min in the air. After complete drying, the sample was placed on the slide glass for the Raman measurements. Then, the ZnPc:Py-PTCDI (1:100)/TSB12/HOPG sample was rinsed 3 times with toluene (0.1 mL × 3) and measured Raman spectrum again. As a reference sample, Py-PTCDI (2 μL, 1.4 μM, 1 equiv., toluene) was drop-casted (~7 × 7 mm^2) onto a TSB12/HOPG and dried for 5 min in the air. After complete drying, the sample was placed on the slide glass for the Raman measurements. After Raman measurement, the Py-PTCDI /TSB12/HOPG sample was rinsed 3 times with toluene (0.1 mL × 3) and measured again.

b) Graphene/quartz substrate: The molecules were deposited on graphene/quartz substrates as the same procedure as HOPG above.

c) Film on slide glass: TSB12 (100 μL, 1 mM, toluene), ZnPc (1 mL, ~50 μM, toluene), and Py-PTCDI (100 μL, 1 mM, toluene) solutions were drop-casted onto clean slide glass (1.2 × 5 cm^2) and slowly dried for 5 min in the air. The thickness of films was ~200 nm.

Computational details: For simulations dedicated to investigate the adsorbed molecule, all geometries were obtained by optimizing the structures at the periodic density functional theory (DFT) level using plane wave combined gaussian approach as implemented in CP2K/Quickstep code.[25-30] A first pre-optimization was always performed at the DFT-B level including a dispersion correction as implemented in CP2K. The final optimization was

carried using the GGA functional PBE along with the Grimme D3 correction to take into account dispersion interaction.[31] The atomic wave functions were expended on double zeta basis set and the auxiliary plane wave basis set for the electron density was truncated at 400 Ry. Due to the large size of the unit cell, all periodic calculations were performed using one k-point (i.e. the Gamma point). STM simulated images were obtained according to the procedure described in Supporting Information.

For calculations performed in solvent, geometries were optimized with the Gaussian16 code,[32] along with the global hybrid functional PBE0.[33] Structural optimizations and subsequent frequency calculations for the ground state were performed using an all electron Pople double zeta basis set with one polarization function on heavier atoms (6-31G(d)). Bulk solvent effects were included using the Polarizable Continuum Model (PCM) of Tomasi and co-workers.[34]

All TD-DFT calculations were carried out with the Gaussian 16 code along with the global hybrid functional PBE0. This functional was chosen because of its frequently reported accuracy for modelling the localized electronic transitions in organic molecules. TD-DFT calculation were performed with the all electron Pople triple zeta basis set with one polarization function on all atoms on heavier atoms, known as 6-311+G(d,p), for H, C, N, O atoms. For the Zn atom, the LANL2DZ pseudopotential and the associated basis set were used.[35] Transitions in absorption were simulated by computing the first 10 transitions in TD-DFT at the same level of theory.

The point charges for the embedded system were obtained by cutting a cluster from the periodic system and pending bonds were saturated by hydrogen atoms. Then, Mulliken charges were computed at AM1 level,[36] and the absorption spectrum of the ZnPc:Py-PTCDI molecule was simulated by embedding the molecule with these point charge. This approach of embedding has proven its accuracy to simulate localized transition in periodic systems.[37] The cluster used for this simulation is presented in Supporting Information (Figure S11).

Supporting Information

Electronic supplementary information (ESI) available.

Conflicts of interest

The authors declare no competing financial interests.

Acknowledgements

This research was supported by Global Research Laboratory (GRL) through the National Research Foundation of Korea (NRF) funded by the Ministry of Science, ICT & Future Planning (2016K1A1A2912753), Brain Pool program funded by the Ministry of Science and ICT through the National Research Foundation of Korea (2018H1D3A2001751), and ANR STACSAMGRAPH project, grant ANR-18-CE09-0030 of the French Agence Nationale de la Recherche. B. K. and E. K. thank Dr. David Kreher (IPCM, Sorbonne Université, France). A.J.A. thanks Dr. Fabrice Charra (CEA Saclay, SPEC, France) for helpful discussions regarding confocal microscopy. The authors thank the SYSPROD project and AXELERA Pôle de Compétitivité for financial support (PSMN Data Center).

References

[1] D. P. Goronzy, M. Ebrahimi, F. Rosei, Arramel, Y. Fang, S. De Feyter, S. L. Tait, C. Wang, P. H. Beton, A. T. S. Wee, P. S. Weiss, D. F. Perepichka, *ACS Nano* **2018**, 12, 7445.

[2] K. S. Mali, N. Pearce, S. De Feyter, N. R. Champness, *Chem. Soc. Rev.* **2017**, 46, 2520.

[3] L. Sosa-Vargas, E. Kim, A.-J. Attias, *Materials Horizons* **2017**, 4, 570.

[4] K. S. Mali, J. Greenwood, J. Adisoejoso, R. Phillipson, S. De Feyter, *Nanoscale* **2015**, 7, 1566.

[5] J. M. MacLeod, F. Rosei, *Small* **2014**, 10, 1038.

[6] A. Ciesielski, P. Samorì, *Adv. Mater.* **2016**, 28, 6030.

[7] V. Georgakilas, J. N. Tiwari, K. C. Kemp, J. A. Perman, A. B. Bourlinos, K. S. Kim, R. Zboril, *Chem. Rev.* **2016**, 116, 5464.

[8] Y. Zhao, S. Ippolito, P. Samori, *Adv. OPtical. Mater.* **2019**, 7, 1900286.

[9] C. J. Lockard de la Rosa, R. Phillipson, J. Teyssandier, J. Adisoejoso, Y. Balaji, C. Huyghebaert, I. Radu, M. Heyns, S. D. Feyter, S. D. Gendt, *Appl. Phys. Lett.* **2016**, 109, 253112.

[10] M. Gobbi, S. Bonacchi, J. X. Lian, Y. Liu, X.-Y. Wang, M.-A. Stoeckel, M. A. Squillaci, G. D'Avino, A. Narita, K. Müllen, X. Feng, Y. Olivier, D. Beljonne, P. Samorì, E. Orgiu, *Nature Communications* **2017**, 8, 14767.

[11] T. H. Phan, H. Van Gorp, Z. Li, T. M. Trung Huynh, Y. Fujita, L. Verstraete, S. Eyley, W. Thielemans, H. Uji-i, B. E. Hirsch, S. F. L. Mertens, J. Greenwood, O. Ivasenko, S. De Feyter, *ACS Nano* **2019**, 13, 5559.

[12] J. Kerfoot, V. V. Korolkov, A. S. Nizovtsev, R. Jones, T. Taniguchi, K. Watanabe, I. Lesanovsky, B. Olmos, N. A. Besley, E. Besley, P. H. Beton, *The Journal of Chemical Physics* **2018**, 149, 054701.

[13] T. Ye, T. Takami, R. Wang, J. Jiang, P. S. Weiss, *J. Am. Chem. Soc.* **2006**, 128, 10984.

[14] T. Ijaz, B. Yang, R. Wang, J. Zhu, A. Farrukh, G. Chen, G. Franc, Y. Zhang, A. Gourdon, Z. Dong, *Appl. Phys. Lett.* **2019**, 115, 173101.

[15] J. A. Mann, J. Rodríguez-López, H. D. Abruña, W. R. Dichtel, *J. Am. Chem. Soc.* **2011**, 133, 17614.

[16] P. Du, M. Jaouen, A. Bocheux, C. Bourgogne, Z. Han, V. Bouchiat, D. Kreher, F. Mathevet, C. Fiorini-Debuisschert, F. Charra, A.-J. Attias, *Angew. Chem. Int. Ed.* **2014**, 53, 10060.

[17] S. Le Liepvre, P. Du, D. Kreher, F. Mathevet, A.-J. Attias, C. Fiorini-Debuisschert, L. Douillard, F. Charra, *ACS Photonics* **2016**, 3, 2291.

[18] R. Brisse, D. Guianvarc'h, C. Mansuy, S. Sagan, D. Kreher, L. Sosa-Vargas, L. Hamitouche, V. Humblot, I. Arfaoui, V. Labet, C. Paris, C. Petit, A.-J. Attias, *Chem. Commun.* **2018**, 54, 10068.

[19] M. J. Robb, B. Newton, B. P. Fors, C. J. Hawker, *The Journal of Organic Chemistry* **2014**, 79, 6360.

[20] J. Visser, N. Katsonis, J. Vicario, B. L. Feringa, *Langmuir* **2009**, 25, 5980.

[21] N. Kalashnyk, M. Jaouen, C. Fiorini-Debuisschert, L. Douillard, A.-J. Attias, F. Charra, *Chem. Commun.* **2018**, 54, 9607.

[22] N. Kalashnyk, A. Gouesmel, E. Kim, A.-J. Attias, F. Charra, *2D Materials* **2019**, 6, 045016.

[23] C. Arrigoni, G. Schull, D. Bléger, L. Douillard, C. Fiorini-Debuisschert, F. Mathevet, D. Kreher, A.-J. Attias, F. Charra, *The Journal of Physical Chemistry Letters* **2010**, 1, 190.

[24] T. Del Caño, J. Duff, R. Aroca, *Appl. Spectrosc.* **2002**, 56, 744.

[25] A. C. Ferrari, *Solid State Commun.* **2007**, 143, 47.

[26] D. Wöll, E. Braeken, A. Deres, F. C. De Schryver, H. Uji-i, J. Hofkens, *Chem. Soc. Rev.* **2009**, 38, 313.

[27] J. VandeVondele, M. Krack, F. Mohamed, M. Parrinello, T. Chassaing, J.Hutter, *Comput. Phys. Commun*. **2005**, 167, 103.

[28] J. VandeVondele, J. Hutter, *J. Chem. Phys*. **2007**, 127, 114105.

[29] G. Lippert, J. Hutter, M. Parrinello, *Mol. Phys*. **1997**, 92, 477.

[30] J. Hutter, M. Iannuzi, F. Schiffmann, J. VandeVondele, *Wiley Interdiscip. Rev. Comput. Mol. Sci.* 2014, 4, 15.

[31] S. Grimme, J. Antony, S. Ehrlich, H. Krieg, *J. Chem. Phys.* **2010**, 132, 154104.

[32] M. J. Frisch, G. W. Trucks, H. B. Schlegel, G. E. Scuseria, M. A. Robb, J. R. Cheeseman, G. Scalmani, V. Barone, G. A. Petersson, H. Nakatsuji, X. Li, M. Caricato, A. V. Marenich, J. Bloino, B. G. Janesko, R. Gomperts, B. Mennucci, H. P. Hratchian, J. V. Ortiz, A.

F. Izmaylov, J. L. Sonnenberg, Williams, F. Ding, F. Lipparini, F. Egidi, J. Goings, B. Peng, A. Petrone, T. Henderson, D. Ranasinghe, V. G. Zakrzewski, J. Gao, N. Rega, G. Zheng, W. Liang, M. Hada, M. Ehara, K. Toyota, R. Fukuda, J. Hasegawa, M. Ishida, T. Nakajima, Y. Honda, O. Kitao, H. Nakai, T. Vreven, K. Throssell, J. A. Montgomery Jr., J. E. Peralta, F. Ogliaro, M. J. Bearpark, J. J. Heyd, E. N. Brothers, K. N. Kudin, V. N. Staroverov, T. A. Keith, R. Kobayashi, J. Normand, K. Raghavachari, A. P. Rendell, J. C. Burant, S. S. Iyengar, J. Tomasi, M. Cossi, J. M. Millam, M. Klene, C. Adamo, R. Cammi, J. W. Ochterski, R. L. Martin, K. Morokuma, O. Farkas, J. B. Foresman, D. J. Fox, Wallingford, CT 2016.

[33] C. Adamo, V. Barone, *The Journal of Chemical Physics* **1999**, 110, 6158.

[34] J. Tomasi, M. Persico, *Chem. Rev.* **1994**, 94, 2027.

[35] P. J. Hay, W. R. Wadt, *The Journal of Chemical Physics* **1985**, 82, 270.

[36] M. J. S. Dewar, E. G. Zoebisch, E. F. Healy, J. J. P. Stewart, *J. Am. Chem. Soc.* **1985**, 107, 3902.

[37] A. Curutchet, T. Le Bahers, *Inorg. Chem.* **2017**, 56, 414.

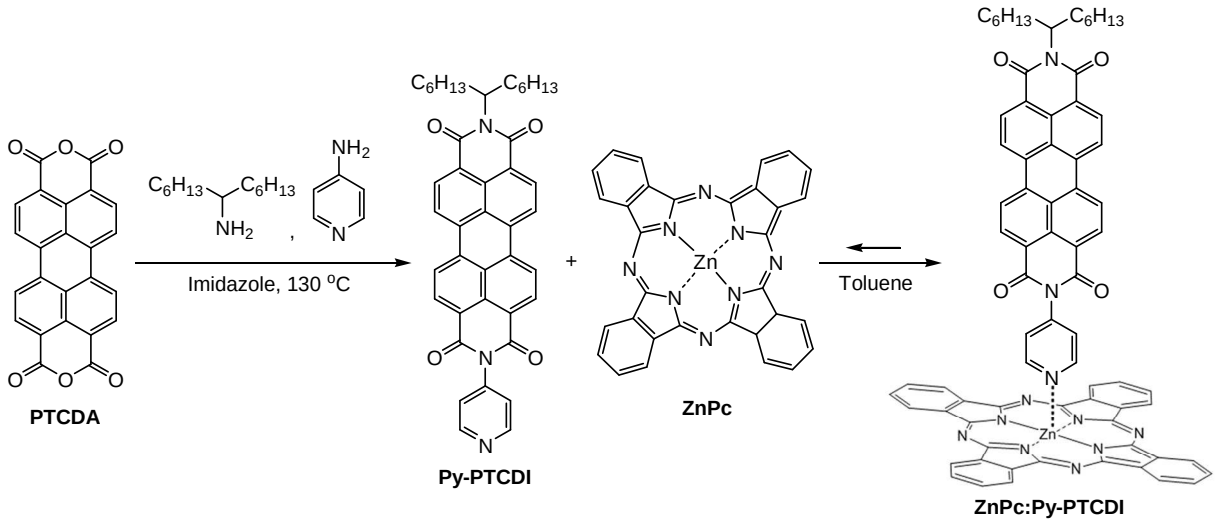

Scheme 1. Molecular structures and synthesis of Py-PTCDI ligand and ZnPc:Py-PTCDI complex.

Table 1. Absorption and emission wavelengths of Py-PTCDI in solution (toluene), film on quartz and excitation and emission wavelengths of the self-assembly (ZnPc:Py-PTCDI onto TSB12 network) on monolayer graphene transferred on quartz.

UV-Vis Absorption and emission				**Confocal microscopy Excitation and emission**	
In solution[a)]		**Film**		**On-graphene self-assembled platform**	
λ_{abs} (nm)	**λ_{em} (nm)**	**λ_{abs} (nm)**	**λ_{em} (nm)**	**λ_{abs} (nm)**	**λ_{em} (nm)**
527	**540**	**545**	**607[b)]**	**526**	**530**
491	**578**	**499**		**490**	**570**
460	**628**	**474**			

[a)] toluene; [b)] structureless broadband

Table 2. TD-DFT computed vertical transitions in absorption for 3 different scenarios (see text for more information) for the transitions localized on the ZnPc and Py-PTCDI moieties at the PBE0/6-311+G(d,p) level. Transitions are given in nm.

Situtation	**(a)** **Geom: gas phase** **Environment : gas phase**	**(b)** **Geom: adsorbed** **Environment : gas phase**	**(c)** **Geom: adsorbed** **Environment : embedded**
ZnPc	**608**	**609**	**610**
Py-PTCDI	**527**	**526**	**526**

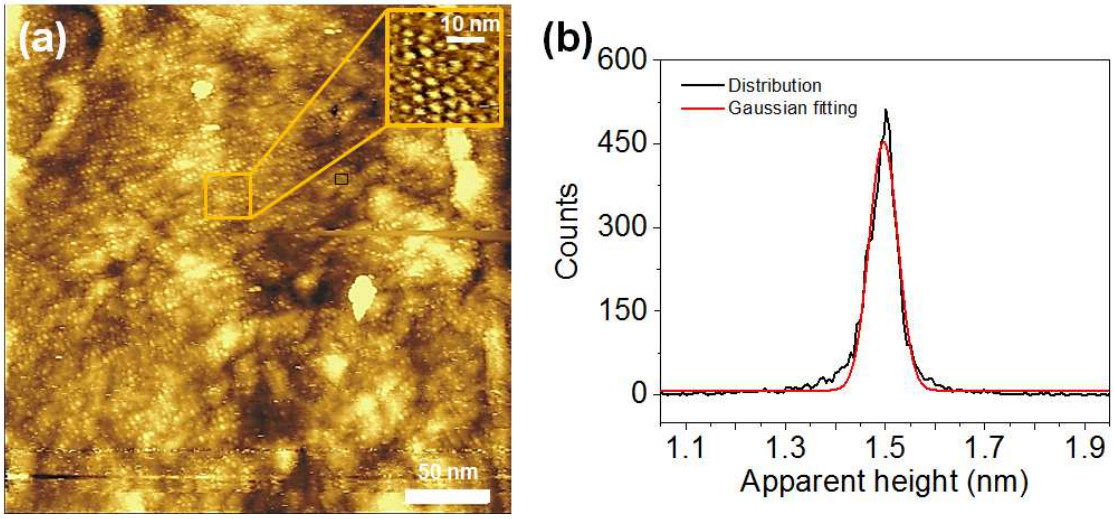

Figure 1. STM images and profiles on graphene. (a) STM image at graphene/phenyloctane interface of the ZnPc:Py-PTCDI (1:100) system drop-casted three times and rinsed, onto the TSB12 honeycomb network. V_{bias}= -1.2 V and I_t= 12 pA. (b) The apparent height distribution and Gaussian fitting profile of the apparent height distribution for the spots on the whole STM image (a). The average distributions is 1.5±0.1 nm, $N(1.50, 0.06^2)$, p=0.95. Inset on (a): the blue triangles indicate the TSB12 and orange dot indicates the ZnPc:Py-PTCDI. Scale bar is 3 nm.

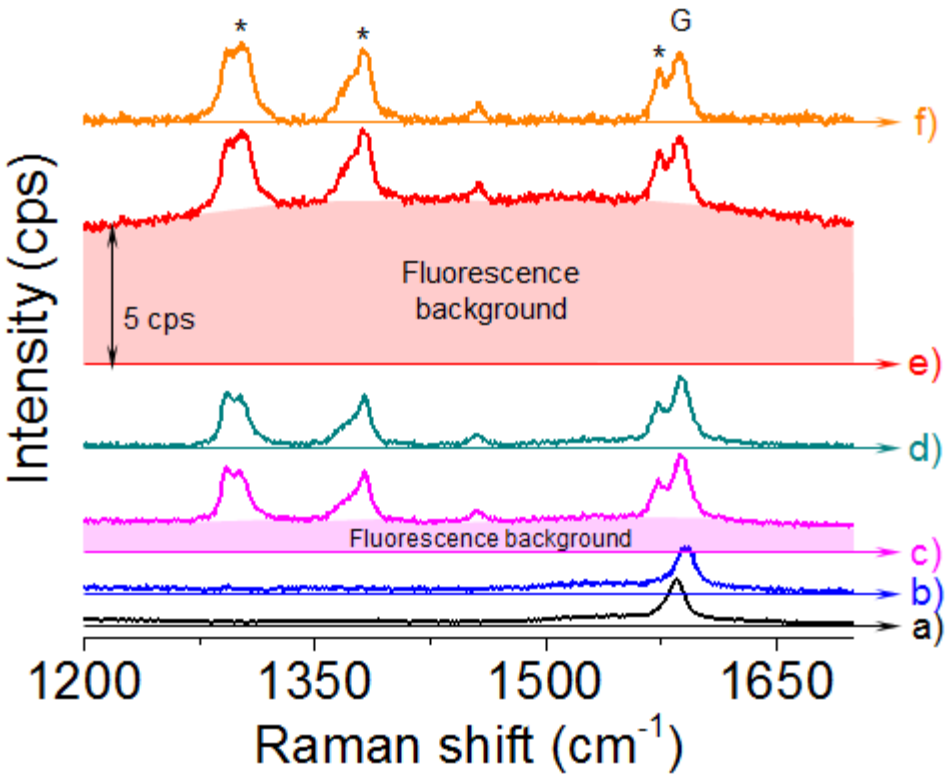

Figure 2. Raman spectra of pristine and functionalized graphene surfaces. (a) Graphene. Graphene with deposits of (b) TSB12, (c-f) subsequent addition of ZnPc:Py-PTCDI (1:100): drop-casted once and rinsed (c) before and (d) after subtracting fluorescence background, drop-casted three times and rinsed (e) before and (f) after subtracting fluorescence background. Asterisks shows the characteristic Raman modes of Py-PTCDI and 'G' stands for the G-mode band of graphene. Laser line iss et at 532 nm. One way arrows indicate the line with zero intensity values for each spectrum.

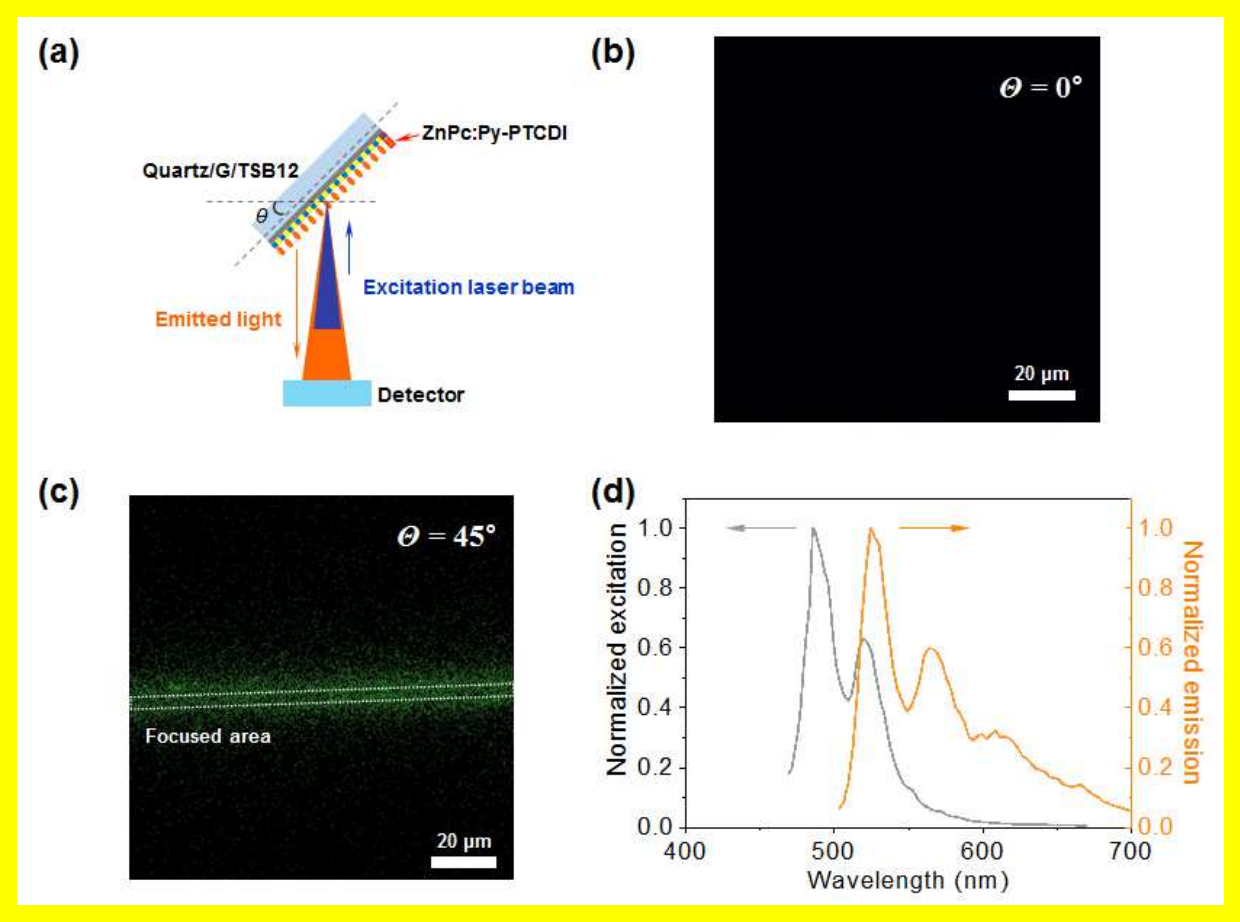

Figure 3. Confocal microscopy. (a) Scheme of principle for the definition of the tilt angle θ. Fluorescence confocal microscopy images (laser beam wavelength = 490 nm) of Graphene/TSB12/ ZnPc:Py-PTCDI system after rinsing, (b) $\theta = 0°$ and (c) $\theta = 45°$. (d) Excitation (λ_{em} = xxx nm) and emission spectra (λ_{ex} = 490 nm) of the sample for $\theta = 45°$.

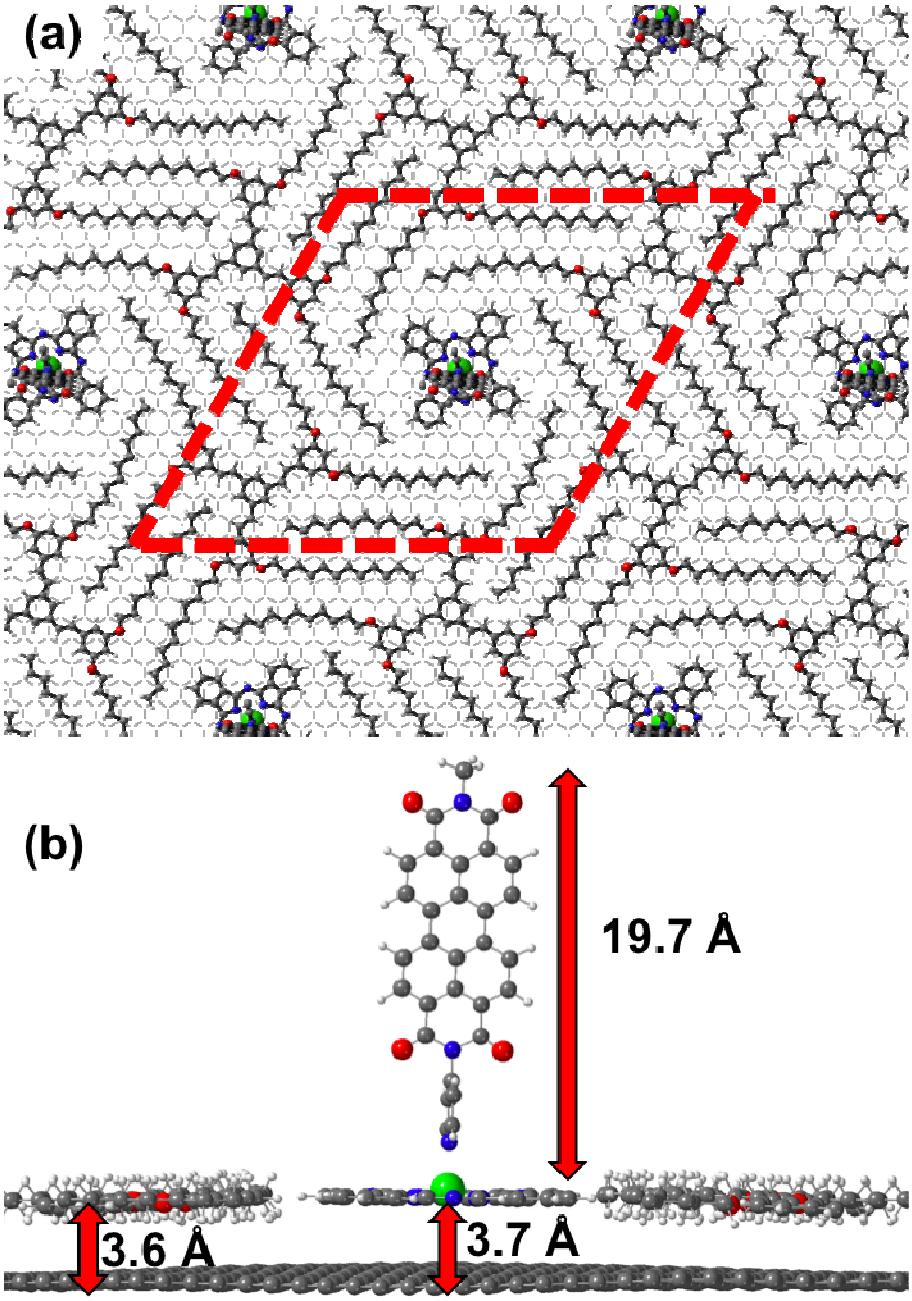

Figure 4. (a) Top and (b) side views of the modelled system made of a graphene layer, covered by TSB12 and ZnPc:Py-PTCDI molecules. The dotted red lines draw the unit cell. Grey, white, blue, red, and green atoms are C, H, N, O and Zn atoms, respectively.